On non-superperfection of edge intersection graphs of paths

Victoria Kaial, Hervé Kerivin, Annegret K Wagler

On non-superperfection of edge intersection graphs of paths

Victoria Kaial[a], Hervé Kerivin[a,1], Annegret K. Wagler[a,1]

[a] *University Clermont Auvergne, LIMOS (UMR 6158 CNRS), Clermont-Ferrand, France*

Abstract

The routing and spectrum assignment problem in modern flexgrid elastic optical networks asks for assigning to given demands a route in an optical network and a channel within an optical frequency spectrum so that the channels of two demands are disjoint whenever their routes share a link in the optical network. This problem can be modeled in two phases: firstly, a selection of paths in the network and, secondly, an interval coloring problem in the edge intersection graph of these paths. The interval chromatic number equals the smallest size of a spectrum such that a proper interval coloring is possible, the weighted clique number is a natural lower bound. Graphs where both parameters coincide for all possible non-negative integral weights are called superperfect. Therefore, the occurence of non-superperfect edge intersection graphs of routing paths can provoke the need of larger spectral ressources. In this work, we examine the question which minimal non-superperfect graphs can occur in the edge intersection graphs of routing paths in different underlying networks: when the network is a path, a tree, a cycle, or a sparse planar graph with small maximum degree. We show that for any possible network (even if it is restricted to a path) the resulting edge intersection graphs are not necessarily superperfect. We close with a discussion of possible consequences and of some lines of future research.

Key words: Routing and spectrum assignment problem, edge intersection graph of paths, interval coloring, superperfection.

1. Introduction

In optical networks, light is used as a communication medium between sending and receiving nodes. That is, we are given a graph $G = (V, E)$ that represents an optical network and a set $\mathcal{D}$ of demands, where each demand $k \in \mathcal{D}$ is specified by

- an origin node $o_k \in V$,
- a destination node $d_k \in V \setminus \{o_k\}$, and
- a weight $w_k \in \mathbb{Z}_+$ as traffic demand.

For over two decades, wavelength-division multiplexing (WDM) has been the most popular technology used in optical networks, where different wavelengths are used to simultaneously transport signals over a single optical fiber. The resulting *routing and wavelength assignment (RWA)*

Email addresses: victoria.kaial@uca.fr (Victoria Kaial), herve.kerivin@uca.fr (Hervé Kerivin), annegret.wagler@uca.fr (Annegret K. Wagler)

[1] This work was supported by the French National Research Agency grant ANR-17-CE25-0006 (FLEXOPTIM).

problem asks to find, for each demand $k \in \mathcal{D}$, a route P_k through the network and a wavelength so that routes with the same wavelength share no edges, and the number of used wavelengths is minimized [18]. However, WDM has to select the wavelengths from a rather coarse fixed grid of frequencies and leads to an inefficient use of spectral resources.

In response to the continuous growth of data traffic volumes, a new generation of optical networks, called flexgrid optical networks, has been introduced to enhance the spectrum efficiency. In such networks, the frequency spectrum of an optical fiber is divided into narrow frequency slots and any sequence of consecutive slots can form a channel on optical fibers. That way, flexgrid optical networks enable capacity gain by allocating minimum required bandwidth to each demand. The resulting *routing and spectrum assignment (RSA)* problem is a generalization of the RWA problem and consists of finding, for each demand $k \in \mathcal{D}$, a route P_k through the network and a channel S_k of w_k consecutive frequency slots so that the channels of two demands are disjoint whenever their routes have an edge in common, and the number of used frequency slots is minimized [21].

The two problems can be reinterpreted in combinatorial terms as follows. A *routing* $\mathcal{P}$ is an assignment of each demand $k \in \mathcal{D}$ to an (o_k, d_k)-path P_k in G. The *edge intersection graph* $I(\mathcal{P})$ of a routing $\mathcal{P}$ has the paths $P_k \in \mathcal{P}$ as nodes and two nodes are joined by an edge if the corresponding paths in G are in conflict as they share an edge (notice that we do not care whether they share nodes). The spectrum assignment of the RSA problem corresponds to an *interval coloring* of $I(\mathcal{P})$ weighted with the traffic demands w_k, that is to an assignment of intervals S_k of w_k consecutive frequency slots to the nodes of $I(\mathcal{P})$ so that the intervals of adjacent nodes are disjoint. Let $\mathbf{w} \in \mathbf{Z}_+^{|\mathcal{D}|}$ be the vector with entry w_k for each demand k in $\mathcal{D}$. The *interval chromatic number* $\chi_I(I(\mathcal{P}), \mathbf{w})$ is the smallest number of frequency slots allowing a proper interval coloring. Given G and $\mathcal{D}$, the minimum spectrum width of any solution of the RSA problem, thus, equals

$$\chi_I(G, \mathcal{D}) = \min\{\chi_I(I(\mathcal{P}), \mathbf{w}) : \mathcal{P} \text{ possible routing of demands } \mathcal{D} \text{ in } G\}.$$

On the other hand, the wavelength assignment of the RWA problem corresponds to a (usual) coloring of $I(\mathcal{P})$ and the minimum number of used wavelengths equals the chromatic number $\chi(I(\mathcal{P})) = \chi_I(I(\mathcal{P}), \mathbf{1})$, with $\mathbf{1} = (1, \ldots, 1)$, taken over all possible routings $\mathcal{P}$ of demands $\mathcal{D}$ in G.

Both problems have been shown to be NP-hard [3, 22]. We note that the RSA problem remains hard even when the network is a path [20], whereas the RWA problem is polynomially solvable in this case [6]. The reason is that the edge intersection graphs of the routings fall into the class of interval graphs when the network is a path - and coloring interval graphs can be done in polynomial time, but finding an optimal interval coloring is already hard in this case, see [8].

This paper is motivated by the RSA problem and the task to determine $\chi_I(G, \mathcal{D})$. For that, we note that for each routing $\mathcal{P}$, the *weighted clique number* $\omega(I(\mathcal{P}), \mathbf{w})$, also taking the traffic demands w_k as weights, equals the weight of a heaviest clique in $I(\mathcal{P}, \mathbf{w})$ and is a natural lower bound for $\chi_I(I(\mathcal{P}), \mathbf{w})$ (as clearly the intervals of all nodes in a clique in $I(\mathcal{P})$ have to be disjoint by the construction of $I(\mathcal{P})$). Thus,

$$\omega(G, \mathcal{D}) = \min\{\omega(I(\mathcal{P}), \mathbf{w}) : \mathcal{P} \text{ possible routing of demands } \mathcal{D} \text{ in } G\}$$

is a lower bound for $\chi_I(G, \mathcal{D})$. However, it is not always possible to find a solution with this lower bound $\omega(G, \mathcal{D})$ as spectrum width, as weighted clique number and interval chromatic number of the edge intersection graphs are not always equal.

Graphs where weighted clique number and interval chromatic number coincide for all possible non-negative integral weights are called *superperfect*.

A graph is *perfect* if and only if this holds for every $(0,1)$-weighting $\mathbf{w}$ of its nodes. According to a characterization achieved by Chudnovsky et al. [4], perfect graphs are precisely the graphs without chordless cycles C_{2k+1} with $k \geq 2$, termed *odd holes*, or their complements, the *odd antiholes* $\overline{C}_{2k+1}$ (the complement $\overline{G}$ has the same nodes as G, but two nodes are adjacent in $\overline{G}$ if and only if they are non-adjacent in G). In particular, every superperfect graph is perfect.

On the other hand, comparability graphs form a subclass of superperfect graphs. A graph $G = (V, E)$ is *comparability* if and only if there exists a partial order $\mathcal{O}$ on $V \times V$ such that $uv \in E$ if and only if u and v are comparable w.r.t. $\mathcal{O}$. Hoffman [13] proved that every comparability graph is superperfect. Gallai [7] characterized comparability graphs by giving the following complete list of minimal non-comparability graphs:

- odd holes C_{2k+1} for $k \geq 2$ and antiholes $\overline{C}_n$ for $n \geq 6$,
- the graphs J_k and J'_k for $k \geq 2$ and the graphs J''_k for $k \geq 3$ (see Fig. 1),
- the complements of D_k for $k \geq 2$ and of E_k and F_k for $k \geq 1$ (see Fig. 2),
- the complements of $A_1, \ldots, A_{10}$ (see Fig. 3).

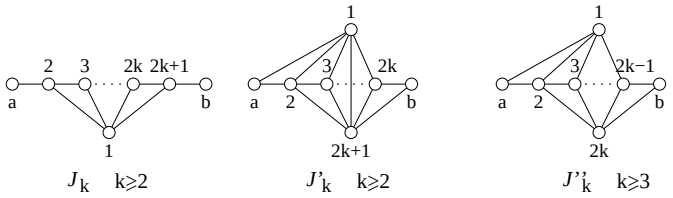

Figure 1: Minimal non-comparability graphs: J_k, J'_k for $k \geq 2$ and J''_k for $k \geq 3$.

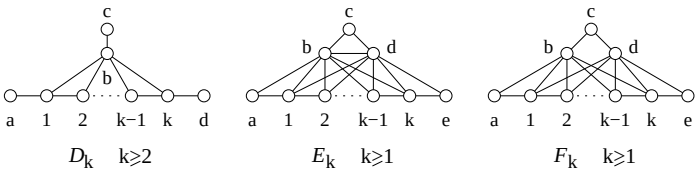

Figure 2: Minimal non-comparability graphs: the complements of D_k, E_k, F_k.

As comparability graphs form a subclass of superperfect graphs, we have that every non-superperfect graph is in particular non-comparability, which raises the question of which minimal non-comparability graphs are also minimal non-superperfect, see Section 2.

In this paper, we examine for different networks G, the question whether or not there is a solution of the RSA problem with $\omega(G, \mathcal{D})$ as spectrum width - which depends on the occurrence of (minimal) non-superperfect graphs in the edge intersection graphs $I(\mathcal{P})$.

For some networks G, the edge intersection graphs form well-studied graph classes: if G is a

- *path*, then $I(\mathcal{P})$ is an *interval graph*,
- *tree*, then $I(\mathcal{P})$ is an *EPT graph* [9],
- *cycle*, then $I(\mathcal{P})$ is a *circular-arc graph*,

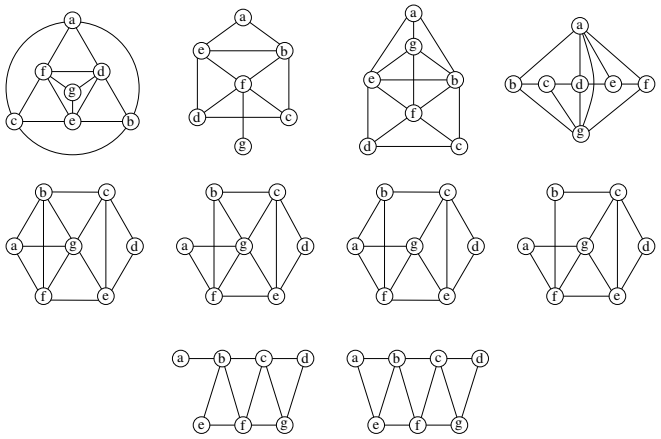

Figure 3: Minimal non-comparability graphs: the graphs $\overline{A}_1, \ldots, \overline{A}_{10}$ (from top left to bottom right).

see Section 3, 4 and 5, resp. However, if G is a sufficiently large grid, then it is known by [10] that $I(\mathcal{P})$ can be *any* graph. Modern optical networks do not fall in any of these classes, but are 2-connected, sparse planar graphs with small maximum degree with a grid-like structure. In accordance with [9], we also refer to interval graphs as *EPP graphs*, to circular-arc graphs as *EPC graphs*, and call edge intersection graphs of paths in an optical network *EPN graphs*.

We first study the cases when the underlying network G is a path, a tree or a cycle (see Section 3, 4 and 5, resp.). We recall results on interval graphs, EPT graphs and circular-arc graphs from [16, 9, 5] and discuss which minimal non-comparability non-superperfect graphs can occur. In addition, we exhibit new examples of minimal non-superperfect graphs within these classes.

All of these non-superperfect graphs are inherited for the case when G is an optical network, and we give also representations as edge intersection graphs for the remaining minimal non-comparability non-superperfect graphs. In view of the result on edge intersection graphs of paths in a sufficiently large grid [10], we expect that any further minimal non-superperfect graph has such a representation and give some further new examples of such graphs.

We close with some concluding remarks and open problems.

Parts of the results, presented hereafter, appeared without proofs in [15].

2. Basic and non-basic minimal non-superperfect graphs

As comparability graphs form a subclass of superperfect graphs [13], we have that every non-superperfect graph is in particular non-comparability, which raises the question of which minimal non-comparability graphs are also minimal non-superperfect. Clearly, odd holes and odd antiholes are minimal non-superperfect (as they are minimal non-perfect [4]). It has been shown by Golumbic [8] that $\overline{A}_1$, $\overline{D}_2$, $\overline{E}_1$, $\overline{E}_2$ and J_2 are non-superperfect, but that there also are superperfect non-comparability graphs such as, for instance, even antiholes $\overline{C}_{2k}$ for $k \geq 3$.

Furthermore, Andreae showed in [1], that the graphs J''_k for $k \geq 3$ and the complements of $A_3, \ldots, A_{10}$ are superperfect, but that the graphs J_k for $k \geq 2$ and J'_k for $k \geq 3$ as well as the complements of D_k for $k \geq 2$ and of E_k, F_k for $k \geq 1$ are non-superperfect.

Note that Andreae wrongly determined $\overline{A}_2$ as superperfect which is, in fact, not the case (see Fig. 4 for a weight vector $\mathbf{w}$ and an optimal interval coloring showing that $\omega(\overline{A}_2, \mathbf{w}) = 5 < 6 = \chi_I(\overline{A}_2, \mathbf{w})$ holds).

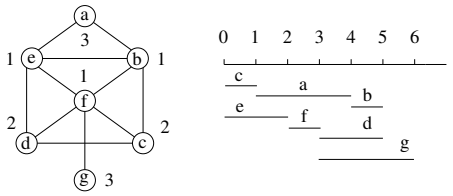

Figure 4: The non-superperfect graph $\overline{A}_2$ together with node weights $\mathbf{w}$ and an optimal interval coloring showing $\omega(\overline{A}_2, \mathbf{w}) = 5 < 6 = \chi_I(\overline{A}_2, \mathbf{w})$.

Moreover, Andreae wrongly determined J_2' as non-superperfect which is, in fact, not the case.

Lemma 1. *J_2' is a superperfect graph.*

Proof. Consider the graph J_2' shown in Fig. 5. We denote by $I(v)$ the interval assigned to node v. In order to show that $\omega(J_2', \mathbf{w}) = \chi_I(J_2', \mathbf{w})$ holds for all non-negative integral node weights $\mathbf{w}$, we distinguish the following two cases.

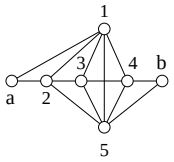

Figure 5: The superperfect graph J_2'.

Case 1. *$Q_1 = \{a, 1, 2\}$ is a maximum weight clique of $(J_2', \mathbf{w})$.*

Then we have $\omega = \omega(J_2', \mathbf{w}) = w_a + w_1 + w_2$.
If $w_4 > w_2$, then there is a feasible interval coloring of width ω:

- let $I(1) = [0, w_1)$, $I(a) = [w_1, w_1 + w_a)$ and $I(2) = [w_1 + w_a, \omega)$,
- $w_3 + w_5 \leq w_a$ (as Q_1 has maximum weight) and a being non-adjacent to 3,5 allows $I(3) \cup I(5) \subseteq I(a)$,
- with $I(3) = [w_1, w_1 + w_3)$ and $I(4) = [\omega - w_4, \omega)$, we see that $I(5) = [\omega - w_4 - w_5, \omega - w_4)$ is possible since $w_1 + w_3 + w_5 + w_4 \leq \omega$ (as Q_1 has maximum weight) and 4 is non-adjacent to a and 2,
- $I(b) = [0, w_b)$ is possible since $w_b + w_5 + w_4 \leq \omega$ (as Q_1 has maximum weight) and b is non-adjacent to a, 1, and 3.

If $w_4 \leq w_2$, then there is a feasible interval coloring of width ω:

- let $I(2) = [0, w_2)$, $I(1) = [w_2, w_2 + w_1)$ and $I(a) = [w_2 + w_1, \omega)$,

- $I(3) \cup I(5) \subseteq I(a)$ is again possible,
- $I(4) \subseteq I(2)$ is possible by $w_4 \leq w_2$ and 4 is non-adjacent to 2,
- with $I(4) = [0, w_4)$ and $I(5) = [\omega - w_5, \omega)$, we see that $I(b) = [w_4, w_4 + w_b)$ is clearly possible since $w_b + w_5 + w_4 \leq \omega$ (as Q_1 has maximum weight) and b is non-adjacent to a, 1, 2, and 3.

Case 2. *$Q_2 = \{1, 2, 3, 5\}$ is a maximum weight clique of $(J_2', \mathbf{w})$.*

We have $\omega = \omega(J_2', \mathbf{w}) = w_1 + w_2 + w_3 + w_5$ and there is a feasible interval coloring of width ω:

- let $I(2) = [0, w_2)$, $I(1) = [w_2, w_2 + w_1)$, $I(3) = [w_2 + w_1, \omega - w_5)$ and $I(5) = [\omega - w_5, \omega)$,
- $w_3 + w_5 \geq w_a$ (as Q_2 has maximum weight) and a being non-adjacent to $3, 5$ allows $I(a) \subseteq I(3) \cup I(5)$, say $I(a) = [\omega - w_a, \omega)$,
- 4 non-adjacent to $1, 2$ allows $I(4) = [0, w_4)$,
- $I(b) = [w_4, w_4 + w_b)$ is possible since $w_b + w_5 + w_4 \leq \omega$ (as Q_2 has maximum weight) and b is non-adjacent to a, 1, 2, and 3.

The case with $\{1, 3, 4, 5\}$ maximum weight clique is symmetric to Case 2, whereas the case with $\{4, 5, b\}$ maximum weight clique is symmetric to Case 1. Hence, we have in any case (i.e., for all non-negative integral node weights $\mathbf{w}$) a feasible interval coloring of width $\omega(J_2', \mathbf{w})$. □

Hence, all previous results from [1, 4, 7, 8, 13] together with Lemma 1 imply the following:

Corollary 2. *The following minimal non-comparability graphs are also minimal non-superperfect:*

- *$\overline{A}_1$ and $\overline{A}_2$,*
- *odd holes C_{2k+1} and odd antiholes $\overline{C}_{2k+1}$ for $k \geq 2$,*
- *the graphs J_k for $k \geq 2$ and J_k' for $k \geq 3$ as well as*
- *the complements of D_k for $k \geq 2$ and of E_k, F_k for $k \geq 1$.*

Note that we have $\omega(G, \mathbf{1}) < \chi_I(G, \mathbf{1})$ if G is an odd hole or an odd antihole (as they are not perfect), whereas the other minimal non-superperfect graphs are perfect and, thus, $\omega(G, \mathbf{w}) < \chi_I(G, \mathbf{w})$ is attained for some $\mathbf{w} \neq \mathbf{1}$ (see Fig. 4).

We call a minimal non-superperfect graph *basic* if it is minimal non-comparability, and *non-basic* otherwise. We note that every non-basic minimal non-superperfect graph can neither be imperfect nor a comparability graph. To find non-basic minimal non-superperfect graphs, we can thus make use of the aforementioned complete list of minimal non-comparability graphs found by [7]. Thus, among the graphs with n nodes, the candidates to be non-basic minimal non-superperfect graphs are all graphs that

- are perfect (i.e., do not contain odd holes or odd antiholes),
- do not contain any minimal non-superperfect graph with $\leq n$ nodes, and
- contain a minimal non-comparability superperfect graph with $< n$ nodes, i.e., $\overline{A}_3, \ldots, \overline{A}_{10}$, an even antihole $\overline{C}_{2k}$ for $k \geq 3$, J_2', or a graph J_k'' for $k \geq 3$.

To certify non-superperfection of a graph G, it suffices to exhibit one weight vector $\mathbf{w}$ with $\omega(G, \mathbf{w}) < \chi_I(G, \mathbf{w})$. To test this property, we can use a result from [17] to decide whether a given graph G with weights $\mathbf{w}$ has a feasible interval coloring within a spectrum $[0, s]$. For that, variables l_i, r_i for all nodes i of G encode the interval bounds for $I(i) = [l_i, r_i)$, order variables $x_{ij} \in \{0, 1\}$ for all edges ij of G with $i < j$ encode whether or not the interval $I(i)$ is before $I(j)$.

Due to [17], the following integer linear program has a feasible solution if and only if $(G, \mathbf{w})$ has a feasible interval coloring within a spectrum $[0, s]$:

$$\begin{array}{rcll} w_i & = & r_i - l_i & \forall i \in V \\ 0 & \leq & l_i \leq r_i \leq s & \forall i \in V \\ r_i & \leq & l_j + s(1 - x_{ij}) & \forall ij \in E,\ i < j \\ r_j & \leq & l_i + s x_{ij} & \forall ij \in E,\ i < j \\ x_{ij} & \in & \{0, 1\} & \forall ij \in E,\ i < j \\ l_i,\ r_i & \in & \mathbb{Z} & \forall i \in V \end{array}$$

Hence, we can certify non-superperfection of a graph G if there exists one weight vector $\mathbf{w}$ so that the above integer linear program is infeasible for $s = \omega(G, \mathbf{w})$ in order to find non-basic minimal non-superperfect graphs.

3. EPP graphs: If the network is a path

If the optical network G is a path, then there exists exactly one (o_k, d_k)-path P_k in G for every demand $k = (o_k, d_k, w_k)$ between a pair o_k, d_k of nodes. Hence, if G is a path, then $\mathcal{P}$ and $I(\mathcal{P})$ are uniquely determined for any set $\mathcal{D}$ of demands, and the RSA problem reduces to the spectrum assignment part. The edge intersection graph $I(\mathcal{P})$ of the (unique) routing $\mathcal{P}$ of the demands is an *interval graph* (i.e., the intersection graph of intervals in a line, here represented as subpaths of a path and, thus, also called EPP graphs).

Interval graphs are known to be perfect [2]. In order to examine which basic minimal non-superperfect graphs are interval graphs, we rely on a characterization of minimal non-interval graphs from [16].

A graph is *triangulated* if it does not have holes C_k with $k \geq 4$ as induced subgraphs. Interval graphs are triangulated [12] hence all holes are, in particular, minimal non-interval graphs.

Theorem 3. *If $\mathcal{P}$ is a set of paths in a* path*, then $I(\mathcal{P})$ is an* EPP graph *and can contain J_k for all $k \geq 2$, J'_k for all $k \geq 3$, and $\overline{E}_2$, but none of the other basic minimal non-superperfect graphs.*

Proof. In order to prove the theorem, we present according path collections for the affirmative cases (see Fig. 6 for $\overline{E}_2$ and Claim 1 and 2 for J_k and J'_k, resp.) and exhibit a minimal non-interval graph as induced subgraph in the other basic minimal non-superperfect graphs (see Claim 3).

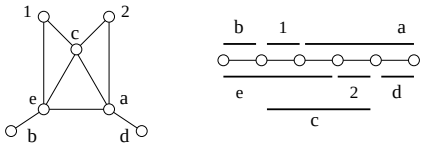

Figure 6: The EPP graph $\overline{E}_2 = I(\mathcal{P})$ with $\mathcal{P}$ in a path.

Claim 1. *$I(\mathcal{P})$ can contain the graphs J_k for all $k \geq 2$.*

Recall from Fig. 1 that J_k is composed of a path $a, 2, \ldots, 2k+1, b$ and that node 1 is adjacent to $2, \ldots, 2k+1$, but not to a and b. We can embed a collection $\mathcal{P}$ of paths $P(i)$ with $I(\mathcal{P}) = J_k$ in a path P_{2k+2} with edges $e_1, e_2, \ldots, e_{2k}, e_{2k+1}$ in such a way that

- $P(a)$ consists of edge e_1, $P(b)$ of edge e_{2k+1},
- $P(1)$ consists of $e_2, \ldots, e_{2k}$, and
- $P(i)$ consists of edges e_{i-1}, e_i for all $2 \leq i \leq 2k+1$.

Thus, for any $k \geq 2$, we have $I(\mathcal{P}) = J_k$, see Fig. 7 for illustration. $\Diamond$

Claim 2. *$I(\mathcal{P})$ can contain the graphs J'_k for all $k \geq 2$.*

Recall from Fig. 1 that J'_k is composed of a path $a, 2, \ldots, 2k, b$, node 1 is adjacent to $a, 2, \ldots, 2k$ and $2k+1$ but not to b, node $2k+1$ is adjacent to 1 and $2, \ldots, 2k, b$ but not to a. We can embed a set $\mathcal{P}$ of paths $P(i)$ with $I(\mathcal{P}) = J'_k$ in a path P_{2k+1} with edges $e_1, e_2, \ldots, e_{2k-1}, e_{2k}$ so that

- $P(a)$ consists of edge e_1, $P(b)$ of edge e_{2k},
- $P(i)$ consists of edges e_{i-1}, e_i for all $2 \leq i \leq 2k$, and
- $P(1)$ consists of edges $e_1, \ldots, e_{2k-1}$, and $P(2k+1)$ of edges $e_2, \ldots, e_{2k-1}, e_{2k}$.

Thus, for any $k \geq 2$, we have $I(\mathcal{P}) = J'_k$, see Fig. 7 for illustration. $\Diamond$

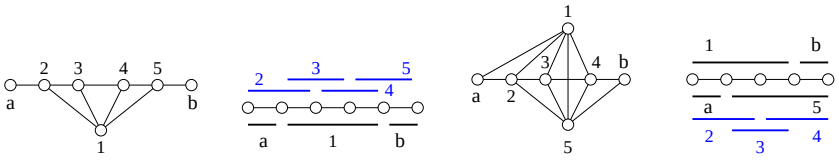

Figure 7: The EPP graphs $J_2 = I(\mathcal{P})$ (on the left) and $J'_2 = I(\mathcal{P})$ (on the right) with $\mathcal{P}$ in a path.

Claim 3. *$I(\mathcal{P})$ can neither contain $\overline{A}_1$, $\overline{A}_2$, nor any odd hole or odd antihole, nor any of the graphs $\overline{D}_k$ for $k \geq 2$, $\overline{E}_k$ for $k \neq 2$, $\overline{F}_k$ for $k \geq 1$.*

Due to [16], odd holes and $\overline{D}_2$, $\overline{E}_1$ are minimal non-interval graphs. The remaining basic minimal non-superperfect graphs contain a C_4 (which is a minimal non-interval graph by [16]):

- every odd antihole $\overline{C}_{2k+1}$ for $k \geq 3$ (induced by the nodes $1, 2, 4, 5$),
- every $\overline{D}_k$ for $k \geq 3$ (induced by the nodes $a, 1, k, d$, see Fig. 2),
- every $\overline{E}_k$ for $k \geq 3$ (induced by the nodes $a, 1, k, e$, see Fig. 2),
- every $\overline{F}_k$ for $k \geq 1$ (induced by the nodes $1, b, c, d$, see Fig. 2),
- $\overline{A}_1$ (induced by a, b, e, f) and $\overline{A}_2$ (induced by e, b, c, d), see Fig. 3.

Hence, none of them is an interval graph. $\square$

Theorem 3 and Corollary 2 imply that EPP graphs are not necessarily superperfect. We next discuss which non-basic minimal non-superperfect graphs can be EPP graphs. Recall that all of them have to contain a minimal non-comparability superperfect graph as proper induced subgraph.

Lemma 4. *An EPP graph can contain $\overline{A}_9$, $\overline{A}_{10}$ and J'_2, but none of the other minimal non-comparability superperfect graphs.*

Proof. Recall that every interval graph is triangulated and, thus, C_4-free. This excludes the occurrence of

- even antiholes $\overline{C}_{2k}$ for $k \geq 3$ (as they all contain a C_4 induced by $1, 2, 4, 5$),
- the graphs J''_k for all $k \geq 3$ (as they all contain a C_4 induced by $1, 2, 2k-1, 2k$),
- the graphs $\overline{A}_3, \ldots \overline{A}_8$ (as they all contain a C_4, see Fig. 3).

On the other hand, there are path representations for the remaining three minimal non-comparability superperfect graphs $\overline{A}_9$, $\overline{A}_{10}$ and J'_2, see Fig. 8 for $\overline{A}_9$, $\overline{A}_{10}$ and Fig. 7 for J'_2. □

Fig. 8 shows non-basic minimal non-superperfect EPP graphs G and G' containing $\overline{A}_9$ and $\overline{A}_{10}$, resp.: they are non-superperfect (due to the indicated weight vectors causing a gap between weighted clique and interval chromatic number), they are minimal (as they do not have a non-comparability subgraph different from $\overline{A}_9 = G - h$ and $\overline{A}_{10} = G' - h$, resp.), they are EPP graphs (see the according path representations).

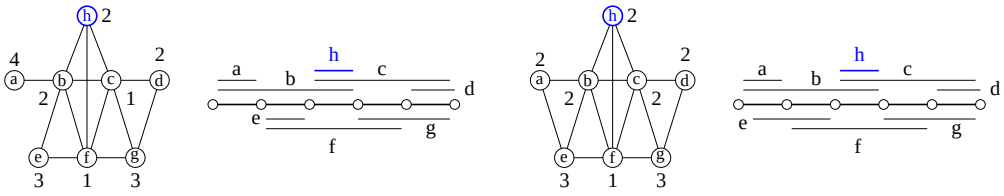

Figure 8: Non-basic minimal non-superperfect EPP graphs G (on the left) and G' (on the right) containing $\overline{A}_9 = G - h$ and $\overline{A}_{10} = G' - h$, resp.

4. EPT graphs: If the network is a tree

If the optical network G is a tree, then there is also exactly one (o_k, d_k)-path P_k in G for every demand $k = (o_k, d_k, w_k)$ between a pair o_k, d_k of nodes. Hence, if G is a tree, then $\mathcal{P}$ and $I(\mathcal{P})$ are uniquely determined for any set of demands, and the RSA problem again reduces to the spectrum assignment part. Edge intersection graphs of paths in trees have been studied in [9] and are called EPT graphs. We recall results from [9] on holes in EPT graphs and examine which minimal non-superperfect graphs can occur in such graphs.

It is known from [9] that EPT graphs are not necessarily perfect as they can contain odd holes. More precisely, Golumbic and Jamison showed the following:

Theorem 5 (Golumbic and Jamison [9]). *If the edge intersection graph $I(\mathcal{P})$ of a collection $\mathcal{P}$ of paths in a tree T contains a hole C_k with $k \geq 4$, then T contains a star $K_{1,k}$ with nodes $b, a_1, \ldots, a_k$ and there are k paths $P_1, \ldots, P_k$ in $\mathcal{P}$ such that P_i precisely contains the edges ba_i and ba_{i+1} of this star (where indices are taken modulo k).*

Figure 9 illustrates the case of $C_5 = I(\mathcal{P})$. From the above result, Golumbic and Jamison deduced the possible adjacencies of a hole which further implies that several graphs cannot occur as induced subgraphs of EPT graphs, including the complement of the P_6 and the two graphs G_1 and G_2 shown in Figure 10. That $\overline{P}_6$ is a non-EPT graph shows particularly that no antihole $\overline{C}_k$ for $k \geq 7$ can occur in such graphs. This implies that an EPT graph is perfect if and only if it

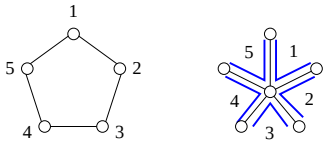

Figure 9: The odd hole $C_5 = I(\mathcal{P})$ with $\mathcal{P}$ in a star.

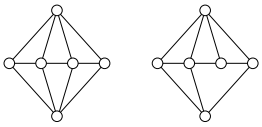

Figure 10: The non-EPT graphs G_1 (on the left) and G_2 (on the right).

does not contain an odd hole. In view of Theorem 5, this is clearly the case when the underlying tree has maximum degree 4, as noted in [9].

Based on the above results, we further examine which basic minimal non-superperfect graphs can occur in edge intersection graphs of paths in a tree:

Theorem 6. *If $\mathcal{P}$ is a set of paths in a* tree*, then the EPT graph $I(\mathcal{P})$ can contain $\overline{A}_1$, $\overline{A}_2$,*

- *odd holes C_{2k+1} for $k \geq 2$, but no odd antiholes $\overline{C}_{2k+1}$ for $k \geq 3$,*
- *the graphs J_k for all $k \geq 2$ and J'_k for all $k \geq 3$, and*
- *$\overline{D}_2$, $\overline{D}_3$, $\overline{E}_1$, $\overline{E}_2$, $\overline{E}_3$, $\overline{F}_1$, $\overline{F}_2$, $\overline{F}_3$, but none of $\overline{D}_k$, $\overline{E}_k$, $\overline{F}_k$ for $k \geq 4$.*

Proof. If $\mathcal{P}$ is a set of paths in a tree, then $I(\mathcal{P})$ can clearly contain

- odd holes C_{2k+1} for $k \geq 2$, but no odd antiholes $\overline{C}_{2k+1}$ for $k \geq 3$ due to [9],
- the graphs J_k for all $k \geq 2$, J'_k for all $k \geq 3$, and $\overline{E}_2$ (as they are, by Theorem 3, examples of interval graphs, which form by construction a subclass of EPT graphs).

For the remaining affirmative cases, we can show:

Claim 4. *$I(\mathcal{P})$ can contain the graphs $\overline{A}_1$, $\overline{A}_2$, $\overline{D}_2$, $\overline{D}_3$, $\overline{E}_1$, $\overline{E}_3$, $\overline{F}_1$, $\overline{F}_2$, $\overline{F}_3$.*

The corresponding collections of paths are shown in Fig. 11 for $\overline{A}_1$, $\overline{A}_2$, Fig. 12 for $\overline{D}_2$ and $\overline{D}_3$, Fig. 13 for $\overline{E}_1$ and $\overline{E}_3$, and Fig. 14 for $\overline{F}_1$, $\overline{F}_2$, and $\overline{F}_3$. $\Diamond$

However, we have:

Claim 5. *$I(\mathcal{P})$ cannot contain the graphs $\overline{D}_k$, $\overline{E}_k$, $\overline{F}_k$ for all $k \geq 4$.*

Recall that $\overline{P}_6$ cannot occur in EPT graphs [9]. Note further that the graphs D_k, E_k, F_k contain a P_6 for all $k \geq 4$ from their definition, see Fig. 2. Thus, $\overline{D}_k$, $\overline{E}_k$, $\overline{F}_k$ have a $\overline{P}_6$ as induced subgraph, and cannot be EPT graphs. $\square$

Theorem 6 and Corollary 2 imply that perfect EPT graphs are not necessarily superperfect.

We next discuss which non-basic minimal non-superperfect graphs can be EPT graphs. Recall that all of them have to be perfect and have to contain a minimal non-comparability superperfect graph as proper induced subgraph.

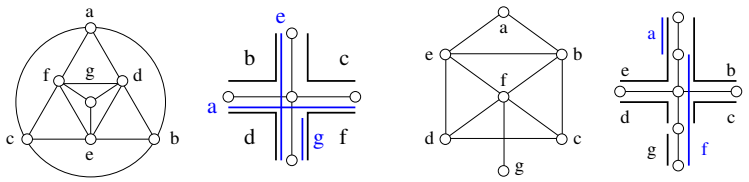

Figure 11: The graphs $\overline{A}_1 = I(\mathcal{P})$ (on the left) and $\overline{A}_2 = I(\mathcal{P})$ (on the right) with $\mathcal{P}$ in a tree.

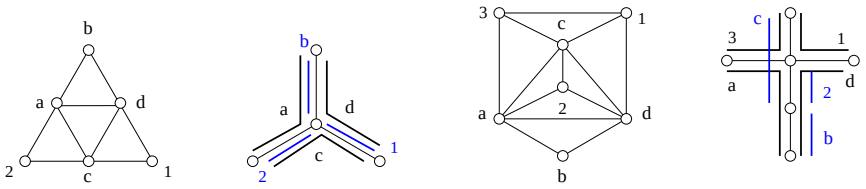

Figure 12: The graphs $\overline{D}_2 = I(\mathcal{P})$ (on the left) and $\overline{D}_3 = I(\mathcal{P})$ (on the right) with $\mathcal{P}$ in a tree.

Lemma 7. *An EPT graph can contain* $\overline{C}_6$, $\overline{A}_3$, $\ldots\overline{A}_6$, $\overline{A}_8$, $\ldots\overline{A}_{10}$ *and* J'_2, *but none of the other minimal non-comparability superperfect graphs.*

Proof. Recall that no EPT graph can contain $\overline{P}_6$ and the two graphs G_1 and G_2, given in Figure 10, as induced subgraph by [9]. This excludes

- even antiholes $\overline{C}_{2k}$ for $k \geq 4$ (as they all contain $\overline{P}_6$),
- the graphs J''_k for all $k \geq 3$ (as they contain G_1 induced by the nodes $1, 2, 3, 4, 5, 2k$), and
- $\overline{A}_7$ (as $\overline{A}_7 - d$ induces a G_2).

On the other hand, $\overline{C}_6$ is an EPT graph [9], J'_2 and $\overline{A}_9$, $\overline{A}_{10}$ are, by Lemma 4, interval graphs which form by construction a subclass of EPT graphs, and it is easy to find path representations as EPT graphs for the remaining minimal non-comparability superperfect graphs $\overline{A}_3$, $\ldots\overline{A}_6$ and $\overline{A}_8$. □

Fig. 15 shows non-basic minimal non-superperfect EPT graphs G and G' containing $\overline{A}_{10}$ resp. $\overline{A}_5$ and J'_2: they are non-superperfect (due to the indicated weight vectors causing a gap between weighted clique and interval chromatic number), they are minimal (as they do not have a non-comparability subgraph different from $\overline{A}_{10} = G - h$ resp. $\overline{A}_5 = G' - h$ and $J'_2 = G' - f$), they are EPT graphs (see the according path representations). However, note that neither G is an interval graph (as it contains a C_4 induced by a, e, f, h) nor G' (as $\overline{A}_5$ is not).

5. EPC graphs: If the network is a cycle

If the optical network G is a cycle, then there exist exactly two (o_k, d_k)-paths P_k in G for every demand $k = (o_k, d_k, w_k)$ between its origin and destination nodes o_k and d_k. Hence, if G is a cycle, then the number of possible routings $\mathcal{P}$ (and their edge intersection graphs $I(\mathcal{P})$) is exponential in the number $|\mathcal{D}|$ of demands, namely $2^{|\mathcal{D}|}$.

Moreover, the edge intersection graphs of paths in a cycle are clearly *circular-arc graphs* (that are the intersection graphs of arcs in a cycle, here represented as paths in a (chordless) cycle and,

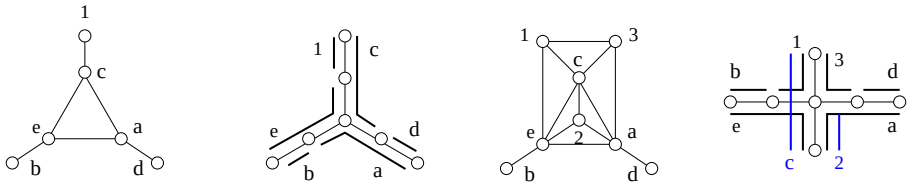

Figure 13: The graphs $\overline{E}_1 = I(\mathcal{P})$ (on the left) and $\overline{E}_3 = I(\mathcal{P})$ (on the right) with $\mathcal{P}$ in a tree.

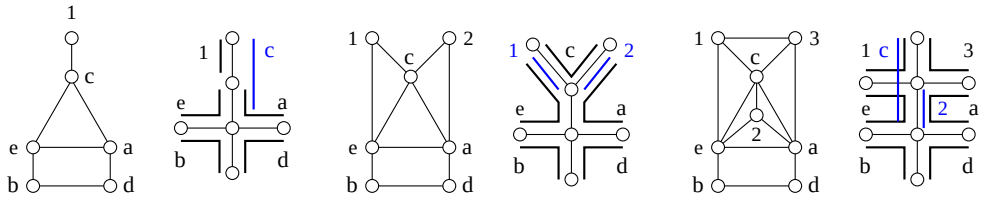

Figure 14: The graphs $\overline{F}_1 = I(\mathcal{P})$ (on the left), $\overline{F}_2 = I(\mathcal{P})$, and $\overline{F}_3 = I(\mathcal{P})$ (on the right) with $\mathcal{P}$ in a tree.

thus, also called EPC graphs). It is well-known that circular-arc graphs are not necessarily perfect as they can contain both odd holes and odd antiholes, see e.g. [5] and Fig. 16 for illustration.

In order to address the question of which of the studied perfect basic minimal non-superperfect graphs can occur in circular-arc graphs, we either present path collections for the affirmative cases or exhibit a minimal non-circular-arc graph otherwise. For that, we first show the following:

Lemma 8. *$\overline{E}_3$ is a minimal non-circular-arc graph.*

Proof. Consider the graph $\overline{E}_3$ shown in Fig. 13. $\overline{E}_3$ contains a C_4 induced by the nodes $1, 3, a, e$. It is well-known that any hole has a unique representation as arcs in a cycle. For this C_4 we obtain paths $P(1) = (1_s, \ldots, 1_t)$, $P(3) = (3_s, \ldots, 3_t)$, $P(a) = (a_s, \ldots, a_t)$, $P(e) = (e_s, \ldots, e_t)$ in a cycle, whose endpoints satisfy in cyclic order $1_s < e_t < 3_s < 1_t < a_s < 3_t < e_s < a_t < 1_s$, see Fig. 17.

For the paths $P(b) = (b_s, \ldots, b_t)$ and $P(d) = (d_s, \ldots, d_t)$, there is only one possibility for each to place them in the cycle:

- as $P(b)$ has to share an edge with $P(e)$ only, we obtain $a_t < b_s < b_t < 1_s$,
- as $P(d)$ has to share an edge with $P(a)$ only, we obtain $3_t < d_s < d_t < e_s$.

Moreover, $P(c) = (c_s, \ldots, c_t)$ must not share an edge with $P(b)$ or $P(d)$, but with each of $P(1), P(3), P(a)$ and $P(e)$ which implies $b_t < c_s < e_t < \ldots < a_s < c_t < d_s$.

Hence, we obtained the paths shown in Fig. 18 as the only possibility to represent $\overline{E}_3 - \{2\}$.

It is left to place the path $P(2)$. According to the adjacencies in $\overline{E}_3$, $P(2)$ has to share an edge with $P(a)$, $P(c)$ and $P(e)$, but with no other path. The edges of the cycle in Fig. 18 marked in bold can be occupied by $P(2)$ (as they satisfy the condition that none of $P(1)$, $P(3)$, $P(b)$, $P(d)$ uses these edges), but none of the subpaths of the cycle composed of bold edges satisfies the condition that it shares an edge with each of $P(a)$, $P(c)$ and $P(e)$.

Hence, $P(2)$ cannot be added to the only possibility to represent $\overline{E}_3 - \{2\}$ and, thus, $\overline{E}_3$ is not a circular-arc graph.

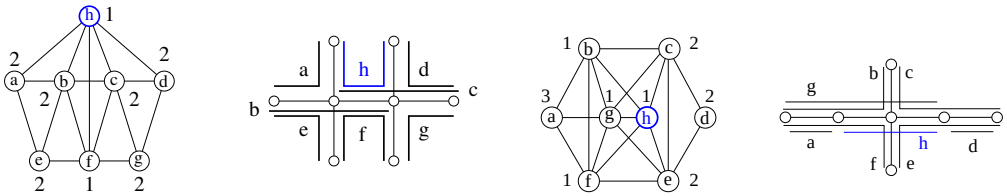

Figure 15: Non-basic minimal non-superperfect EPT graphs G (on the left) and G' (on the right) containing $\overline{A}_{10} = G - h$ resp. $\overline{A}_5 = G' - h$ and $J'_2 = G' - f$

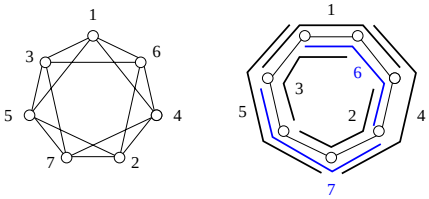

Figure 16: The odd antihole $\overline{C}_7 = I(\mathcal{P})$ with $\mathcal{P}$ in a cycle.

Finally, $\overline{E}_3 - \{v\}$ is a circular-arc graph for any node v. $\overline{E}_3 - \{2\}$ has an according representation, and we can place $P(2)$ whenever we drop the path of one other node:

- removing $P(a)$ enables $P(2) = (c_s, 1_s)$ (as $P(2)$ must not share an edge with $P(a)$ anymore); removing $P(e)$ analogously enables $P(2) = (3_t, c_t)$;
- removing $P(c)$ enables $P(2) = (e_s, a_t)$ (as $P(2)$ does not have to share an edge with $P(c)$ anymore);
- removing $P(b)$ implies that $P(2)$ can occupy the subpath $(e_s, a_t, \ldots, c_s, 1_s)$ and, thus, shares an edge with each of $P(a)$, $P(c)$ and $P(e)$; removing $P(d)$ analogously leads to $P(2) = (3_t, c_t, \ldots, e_s, a_t)$;
- removing $P(1)$ allows to extend $P(a)$, keeping all non-adjacencies, in such a way that $c_s \leq a_s < e_t$ holds which enables $P(2) = (c_s, \ldots, a_s, \ldots, e_t)$; analogously, removing $P(3)$ allows to extend $P(e)$ such that $a_s < e_t \leq c_t$ holds which enables $P(2) = (a_s, \ldots, e_t, \ldots, c_t)$.

Hence, $\overline{E}_3$ is a minimal non-circular-arc graph. □

Making use of the above facts, we can prove:

Theorem 9. *If $\mathcal{P}$ is a set of paths in a* cycle*, then the* EPC graph *$I(\mathcal{P})$ can contain*

- *$\overline{A}_1$ but not $\overline{A}_2$,*
- *all odd holes C_{2k+1} and odd antiholes $\overline{C}_{2k+1}$ for $k \geq 2$,*
- *the graphs J_k for all $k \geq 2$ and J'_k for all $k \geq 3$,*
- *$\overline{D}_2$, $\overline{D}_3$, $\overline{D}_4$, but not the graphs $\overline{D}_k$ for $k \geq 5$,*
- *$\overline{E}_1$ and $\overline{E}_2$, but not the graphs $\overline{E}_k$ for $k \geq 3$, and*
- *$\overline{F}_2$, but not $\overline{F}_1$ neither the graphs $\overline{F}_k$ for $k \geq 3$.*

Proof. If $\mathcal{P}$ is a set of paths in a cycle, then $I(\mathcal{P})$ can clearly contain

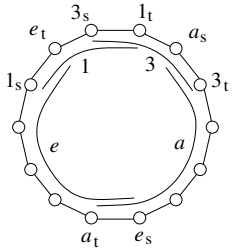

Figure 17: The paths $P(1), P(3), P(a), P(e)$ corresponding to the C_4 induced by the nodes $1, 3, a, e$ in $\overline{E}_3$.

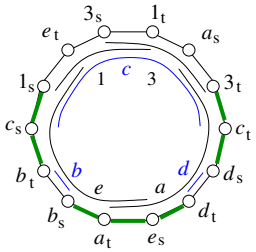

Figure 18: The paths corresponding to the nodes inducing $\overline{E}_3 - \{2\}$.

- odd holes C_{2k+1} and odd antiholes $\overline{C}_{2k+1}$ for $k \geq 2$ (as they are well-known examples of circular-arc graphs, see e.g. [5]),
- the graphs J_k for all $k \geq 2$, J'_k for all $k \geq 3$, and $\overline{E}_2$ (as they are, by Theorem 3, examples of interval graphs, which form by construction a subclass of circular-arc graphs).

For the remaining affirmative cases, we can show:

Claim 6. *The graphs $\overline{A}_1$, $\overline{D}_2$, $\overline{D}_3$, $\overline{D}_4$, $\overline{E}_1$ and $\overline{F}_2$ are circular-arc graphs.*

The corresponding collections of paths are given in Fig. 19 for $\overline{A}_1$ and $\overline{D}_2$, Fig. 20 for $\overline{D}_3$ and $\overline{D}_4$, Fig. 21 for $\overline{E}_1$ and $\overline{F}_2$. $\Diamond$

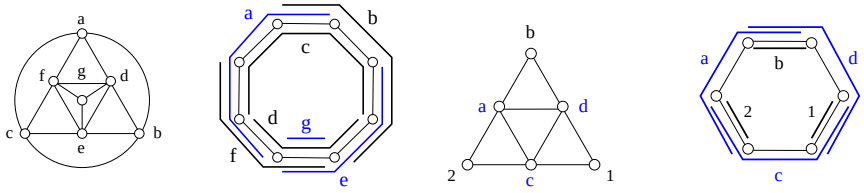

Figure 19: The graphs $\overline{A}_1 = I(\mathcal{P})$ (on the left) and $\overline{D}_2 = I(\mathcal{P})$ (on the right) with $\mathcal{P}$ in a cycle.

However, we have:

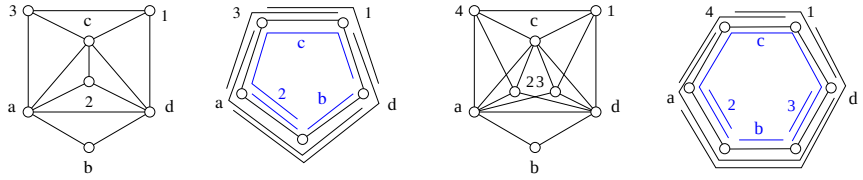

Figure 20: The graphs $\overline{D}_3 = I(\mathcal{P})$ (on the left) and $\overline{D}_4 = I(\mathcal{P})$ (on the right) with $\mathcal{P}$ in a cycle.

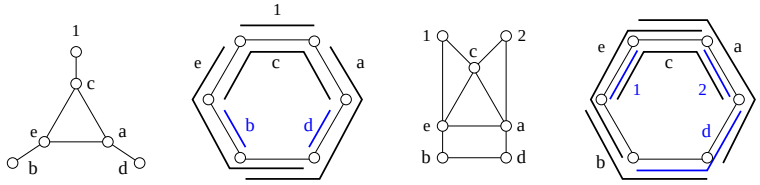

Figure 21: The graphs $\overline{E}_1 = I(\mathcal{P})$ (on the left) and $\overline{F}_2 = I(\mathcal{P})$ (on the right) with $\mathcal{P}$ in a cycle.

Claim 7. *Neither $\overline{A}_2$, $\overline{F}_1$, nor $\overline{F}_k$, $\overline{E}_k$ for $k \geq 3$, nor $\overline{D}_k$ for $k \geq 5$ are circular-arc graphs.*

We have seen in Lemma 8 that $\overline{E}_3$ is not a circular-arc graph. $C_4 \cup K_1$ is a well-known minimal non-circular-arc graph [5]. $C_4 \cup K_1$ occurs as induced subgraph of

- $\overline{A}_2$ (induced by the nodes g and b, c, d, e, see Fig. 4),
- $\overline{F}_1$ (induced by the nodes 1 and a, b, d, e, see Fig. 14),
- each of $\overline{D}_k$ for $k \geq 5$ (induced by the nodes b and $1, 2, k-1, k$, see Fig. 2), and
- each of $\overline{E}_k$ for $k \geq 4$ (induced by the nodes b and $a, 1, k-1, k$, see Fig. 2).

The domino is another well-known minimal non-circular-arc graph [5], and each of $\overline{F}_k$ for $k \geq 3$ contains a domino induced by $1, k, a, b, d, e$ (see $\overline{F}_3$ in Fig. 14 for illustration). □

We next discuss which non-basic minimal non-superperfect graphs can be circular-arc graphs. For that, we first show the following:

Lemma 10. *J_3'' is a minimal non-circular-arc graph.*

Proof. Consider the graph J_3'' shown in Fig. 22. In J_3'', the nodes $a, 2, 3, 4, 5, b$ induce a path

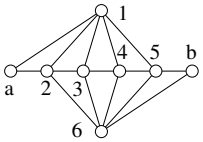

Figure 22: The minimal non-circular-arc graph J_3''.

P_6 which has a unique representation by arcs in a cycle, using paths $P(a) = (a_s, \ldots, a_t)$, $P(2) = (2_s, \ldots, 2_t)$, $P(3) = (3_s, \ldots, 3_t)$, $P(4) = (4_s, \ldots, 4_t)$, $P(5) = (5_s, \ldots, 5_t)$, $P(b) = (b_s, \ldots, b_t)$ in a

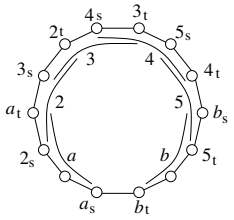

Figure 23: The paths $P(a), P(2), P(3), P(4), P(5), P(b)$ corresponding to the P_6 induced by the nodes $a, 2, 3, 4, 5, b$ in J_3''.

cycle, whose endpoints satisfy in cyclic order $a_s < 2_s < a_t < 3_s < 2_t < 4_s < 3_t < 5_s < 4_t < b_s < 5_t < b_t$, see Fig. 23 for illustration.

For the paths $P(1)$ and $P(6)$, there is only one possibility each. As node 1 is adjacent to $a, 2, 3, 4, 5$ but not to b in J_3'', we get $P(1) = (1_s, \ldots, 1_t)$ with $1_s < a_t < \ldots < 4_t < 1_t < b_s$. As node 6 is adjacent to $2, 3, 4, 5, b$ but not to a in J_3'', we get $P(6) = (6_s, \ldots, 6_t)$ with $a_t < 6_s < 2_t < \ldots < b_s < 5_t < 6_t$. However, this forces $P(1)$ and $P(6)$ to intersect in $3_s \ldots 4_t$, a contradiction as nodes 1 and 6 are not adjacent in J_3''. Hence, J_3'' is not a circular-arc graph.

We have seen that $J_3'' \setminus \{6\}$ (and, symmetrically, also $J_3'' \setminus \{1\}$) has a representation by arcs in a cycle. In order to show that J_3'' is a minimal non-circular-arc graph, it is left to give representations for the remaining proper induced subgraphs. Indeed, there are according representations, see Fig. 24(a) for $J_3'' \setminus \{a\}$ (there is a symmetric representation for $J_3'' \setminus \{b\}$), Fig. 24(b) for $J_3'' \setminus \{2\}$ (symmetric for $J_3'' \setminus \{5\}$), Fig. 24(c) for $J_3'' \setminus \{4\}$ (symmetric for $J_3'' \setminus \{3\}$). □

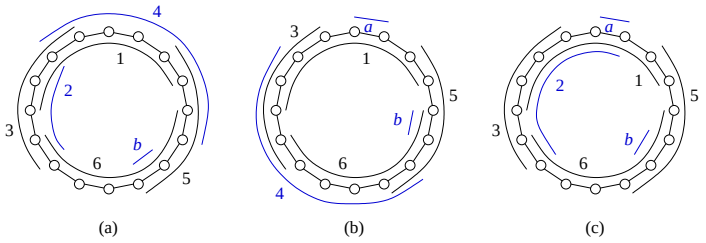

Figure 24: The path representations of (a) $J_3'' \setminus \{a\}$, (b) $J_3'' \setminus \{2\}$, (c) $J_3'' \setminus \{4\}$.

Note that $\overline{E}_3$ and J_3'' are, to the best of our knowledge, *new* examples of minimal non-circular-arc graphs (see, e.g., the results on circular-arc graphs surveyed in [5]).

Finally, recall that every non-basic minimal non-superperfect graph has to be perfect and has to contain a minimal non-comparability superperfect proper induced subgraph.

Lemma 11. *An EPC graph can contain* $\overline{A}_3, \ldots, \overline{A}_{10}$ *and* J_2'*, but none of the other minimal non-comparability superperfect graphs.*

Proof. It is well-known that even antiholes $\overline{C}_{2k}$ for $k \geq 3$ are not circular-arc graphs [5]. Furthermore, J_3'' is not a circular-arc graph (by Lemma 10) and neither are the graphs J_k'' for all $k \geq 4$ (as they all contain the well-known minimal non-circular-arc graph $K_{2,3}$ induced by the nodes $1, 2, 4, 6, 2k$). On the other hand, J_2' and $\overline{A}_9, \overline{A}_{10}$ are, by Lemma 4, interval graphs which form by

construction a subclass of EPC graphs, and it is easy to find path representations as EPC graphs for the remaining minimal non-comparability superperfect graphs $\overline{A}_3, \ldots, \overline{A}_8$. □

Fig. 25 shows non-basic minimal non-superperfect EPC graphs G and G' containing J_2' and $\overline{A}_6$, resp.: they are non-superperfect (due to the indicated weight vectors causing a gap between weighted clique and interval chromatic number), they are minimal (as they do not have a non-comparability subgraph different from $J_2' = G - c$ and $\overline{A}_6 = G' - h$, resp.), they are EPC graphs (see the according path representations). However, note that neither G is an interval graph (as it is the 5-tent which is a minimal non-interval graph by [16]) nor G' (as $\overline{A}_6$ is not).

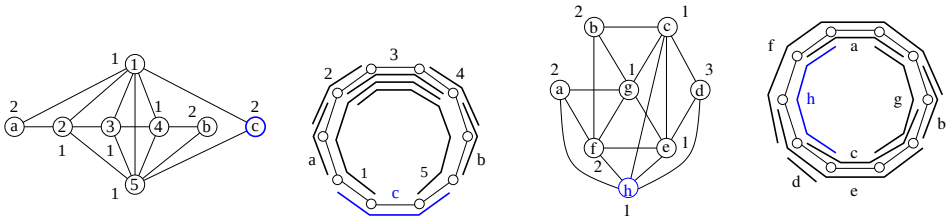

Figure 25: Non-basic minimal non-superperfect EPC graphs G (on the left) and G' (on the right) containing $J_2' = G - c$ and $\overline{A}_6 = G' - h$, resp.

6. EPN graphs: The general case

Modern optical networks have clearly not a tree-like structure neither are just cycles due to survivability aspects concerning node or edge failures in the network G, see e.g. [14]. Instead, today's optical networks are 2-connected, sparse planar graphs with small maximum degree and have more a grid-like structure. As an example, Fig. 26 depicts the Telefónica network of Spain taken from [19].

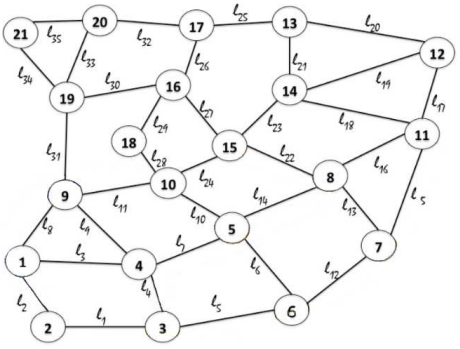

Figure 26: The Telefónica network of Spain from [19].

In view of the result from [10] that *any* graph can be the edge intersection graph of paths in a sufficiently large grid, we expect that also any graph has such a representation in sufficiently

large optical networks. As, however, the construction from [10] makes use of the strong regularity of grids (which does not apply to optical networks), we discuss in the following explicite representations in small sparse graphs. As measure of sparseness, we employ the number of edges that are added to a tree in order to obtain the studied network. A *k-tree* is a graph obtained from a tree by adding exactly k edges. We note that 1-trees form the smallest common superclass of trees and cycles.

We first wonder which basic minimal non-superperfect graphs can occur in edge intersection graphs of paths in such networks G and can show:

Theorem 12. *All minimal non-comparability non-superperfect graphs are EPN graphs and can occur in edge intersection graphs $I(\mathcal{P})$ of sets $\mathcal{P}$ of paths in 1-trees G.*

Proof. In this case, all studied minimal non-superperfect graphs occurring in $I(\mathcal{P})$ when the network G is a tree or a cycle can clearly be present, hence we conclude from Theorem 6 and Theorem 9 that we have

- $\overline{A}_1$ and $\overline{A}_2$ (can occur when G is a tree),
- all odd holes C_{2k+1} for $k \geq 2$ (can occur in both cases),
- all odd antiholes $\overline{C}_{2k+1}$ for $k \geq 2$ (can occur when G is a cycle),
- the graphs J_k for $k \geq 2$ and J'_k for $k \geq 3$ (can occur in both cases),
- the graphs $\overline{D}_2$, $\overline{D}_3$, $\overline{D}_4$ (can occur when G is a cycle), and
- $\overline{E}_1$, $\overline{E}_2$, $\overline{E}_3$, $\overline{F}_1$, $\overline{F}_2$, $\overline{F}_3$ (can occur when G is a tree).

Hence, it is left to address the families $\overline{D}_k$ for $k \geq 5$ and $\overline{E}_k$, $\overline{F}_k$ for $k \geq 4$. We will present the corresponding collections of paths. For that, we first note that the graphs D_k, E_k, F_k contain a P_{k+2} for all $k \geq 4$ from their definition (see Fig. 2), induced by the nodes $a, 1, \ldots, k, d$ in $\overline{D}_k$ and by the nodes $a, 1, \ldots, k, e$ in $\overline{E}_k$, $\overline{F}_k$. Thus, $\overline{D}_k$, $\overline{E}_k$, $\overline{F}_k$ have a $\overline{P}_{k+2}$ which can be represented as circular-arc graph by using the corresponding paths of a path representation of a sufficiently large odd antihole in a cycle C.

We modify this representation in a suitable way and distinguish the following two cases.
Case 1: k is odd and at least 5. Consider a chordless cycle C of size $k+2$ with clockwise-ordered nodes $c_0, c_1, \ldots, c_k, c_{k+1}$ and add a node u being adjacent to c_0 only. Defining $\ell = \frac{k+1}{2}$ and using arithmetics modulo $k+2$, we construct a set $\mathcal{P}'$ consisting of the following paths:

- $P(a) = (u, c_0, c_1, \ldots, c_\ell)$,
- $P(i) = (c_{i\ell}, c_{i\ell+1}, \ldots, c_{i\ell+\ell})$ for $1 \leq i \leq k$,
- $P(d)$ for $\overline{D}_k$ respectively $P(e)$ for $\overline{E}_k$ and $\overline{F}_k$ as $(c_{\ell+1}, c_{\ell+2}, \ldots, c_0, u)$ (note that we have $c_{(k+1)\ell} = c_{\ell+1}$ and $c_{2\ell+1} = c_0$).

By construction, $I(\mathcal{P}')$ is isomorphic to $\overline{P}_{k+2}$. We next choose $P(c) = (c_1, c_2, \ldots, c_{\ell+3})$ to ensure that c is adjacent to all nodes of $\overline{P}_{k+2}$ in the edge intersection graph.

To complete the representation of $\overline{D}_k$, it is only left to choose $P(b) = (u, c_0)$ to ensure that b is adjacent to a and d but to no other node of $\overline{D}_k$.

For $\overline{E}_k$ and $\overline{F}_k$, it remains to find paths $P(b)$ and $P(d)$ sharing an edge with $P(e)$ and $P(a)$ only, respectively. In $\overline{E}_k$, b and d are non-adjacent, hence $P(b)$ and $P(d)$ need to be disjoint. For that, we extend the host graph by two further nodes u_1 and u_2 both being adjacent to u only, extend $P(e)$ by the edge uu_1, $P(a)$ by the edge uu_2, and choose $P(b) = (u, u_1)$ and $P(d) = (u, u_2)$. In $\overline{F}_k$, b and d are adjacent, hence $P(b)$ and $P(d)$ need to share an edge. For that, we extend the

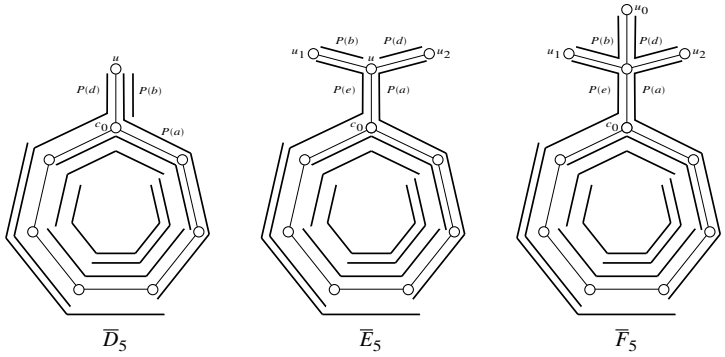

$\overline{D}_5$ $\overline{E}_5$ $\overline{F}_5$

Figure 27: Illustration for the path representation of $\overline{D}_k$, $\overline{E}_k$ and $\overline{F}_k$ for odd $k \geqslant 5$.

host graph by three further nodes u_0, u_1 and u_2 all being adjacent to u only, extend $P(e)$ by the edge uu_1, $P(a)$ by the edge uu_2, and choose $P(b) = (u_0, u, u_1)$ and $P(d) = (u_0, u, u_2)$.

Fig. 27 illustrates the representations of $\overline{D}_k$, $\overline{E}_k$, and $\overline{F}_k$ for $k = 5$.

Case 2: k is even and at least 4. Consider a chordless cycle C of size $k + 3$ with clockwise-ordered nodes $c_0, c_1, \ldots, c_{k+1}, c_{k+2}$ and add nodes v_1, v_2, u and edges c_0v_1, c_0v_2, $c_{\ell+1}u$. Defining $\ell = \frac{k+2}{2}$ and using arithmetics modulo $k + 3$, we construct a set $\mathcal{P}'$ consisting of the following paths:

- $P(a) = (v_2, c_0, c_1, \ldots, c_\ell, c_{\ell+1}, u)$,
- $P(1) = (c_{\ell+1}, c_{\ell+2}, \ldots, c_0, v_1)$,
- $P(2) = (v_2, c_0, c_1, \ldots, c_{\ell-1})$,
- $P(i) = (c_{i\ell}, c_{i\ell+1}, \ldots, c_{i\ell+\ell})$ for $3 \leq i \leq k - 1$,
- $P(k) = (c_{\ell+2}, c_{\ell+3}, \ldots, c_0, v_2)$,
- $P(d)$ for $\overline{D}_k$ respectively $P(e)$ for $\overline{E}_k$ and $\overline{F}_k$ as $(v_1, c_0, c_1, c_2, \ldots c_{l+1}, u)$.

Noting that $P(2)$ and $P(3)$ are disjoint as $\ell - 1 = \frac{k}{2}$ equals $3\ell = \frac{k}{2} + (k + 3)$, $P(k - 1)$ and $P(k)$ are disjoint as $k\ell = (k + 3)\ell - 3\ell \equiv -\frac{k}{2} \equiv \frac{k}{2} + 3 \equiv \ell + 2 (\mathrm{mod} k + 3)$ equals $\ell + 2$, and that $P(1)$ shares edge c_0, v_1 with $P(d)$ respectively $P(e)$, we see that $I(\mathcal{P}')$ is isomorphic to $\overline{P}_{k+2}$ by construction. We next choose $P(c) = (c_l, c_{\ell+1}, c_{\ell+2}, \ldots, c_{2\ell+1} = c_0, v_2)$ to ensure that c is adjacent to all nodes of $\overline{P}_{k+2}$ in the edge intersection graph.

To complete the representation of $\overline{D}_k$, it is only left to choose $P(b) = (c_{\ell+1}, u)$ to ensure that b is adjacent to a and d but no other node of $\overline{D}_k$. For $\overline{E}_k$ and $\overline{F}_k$, we add to the host graph nodes u_1, u_2, respectively u_0, u_1, u_2, all adjacent to u only, and finally extend $P(e)$ and $P(a)$ and define the remaining paths in exactly the same way as in Case 1.

Fig. 28 illustrates the representations of $\overline{D}_k$, $\overline{E}_k$, and $\overline{F}_k$ for $k = 4$.

Hence, the families $\overline{D}_k$ for $k \geq 5$ and $\overline{E}_k$, $\overline{F}_k$ for $k \geq 4$ have representations as edge intersection graphs of paths in a 1-tree. This finally proves the theorem. □

We illustrate this situation with the help of an example.

Example 13. *We consider the Telefónica network of Spain together with its demands as a real instance of the RSA problem (taken from [19]), see Fig. 26 for the network and Table 1 for the set of demands. A natural routing $\mathcal{P}$ (along shortest paths, see again Table 1) yields an edge intersection graph $I(\mathcal{P})$ that contains several minimal non-superperfect graphs, e.g.*

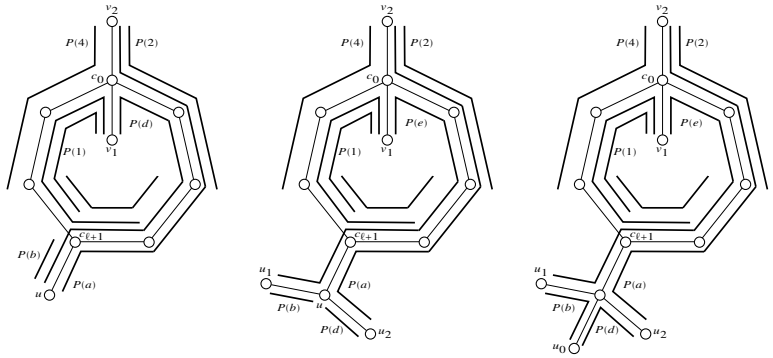

Figure 28: Illustration for the path representations of $\overline{D}_k$, $\overline{E}_k$ and $\overline{F}_k$ for even $k \geqslant 4$.

- *a* C_5 *induced by the paths* P_3, P_{18}, P_{11}, P_{10}, P_{17},
- *a* $\overline{D}_2$ *induced by the paths* P_{16}, P_{12}, P_{11}, P_{15}, P_4, P_{10},
- *a* $\overline{E}_1$ *induced by the paths* P_{16}, P_{11}, P_4, P_1, P_{14}, P_8,
- *a* $\overline{F}_1$ *induced by the paths* P_7, P_{20}, P_{11}, P_5, P_4, P_{14},
- *a* C_7 *induced by the paths* P_{13}, P_{14}, P_{17}, P_{15}, P_{18}, P_{11}, P_{20}, *and*
- *a* J_2 *induced by the paths* P_{16}, P_{12}, P_4, P_{17}, P_8, P_{19}, P_{15}.

Note that, taking the node weights $\mathbf{w}$ *into account, there are indeed gaps between the weighted clique number and the interval chromatic number for the two odd holes* C_5 *and* C_7.

In addition, there are non-basic minimal non-superperfect graphs in edge intersection graphs of paths in networks. We first show:

Lemma 14. *All minimal non-comparability superperfect graphs are EPN graphs and can occur in edge intersection graphs* $I(\mathcal{P})$ *of sets* $\mathcal{P}$ *of paths in optical networks* G.

Proof. In this case, all studied minimal non-comparability superperfect graphs occurring in $I(\mathcal{P})$ when the network G is a tree or a cycle can clearly be present. Hence we conclude from Lemma 7 and Lemma 11 that $I(\mathcal{P})$ can contain

- the even antihole $\overline{C}_6$ (when G is a tree),
- the graph J_2' (in both cases), and
- the graphs $\overline{A}_3$, ..., $\overline{A}_{10}$ (when G is a cycle).

Hence, it is left to address the two remaining families, i.e., even antiholes $\overline{C}_{2k}$ for $k \geq 4$ and the graphs J_k'' for all $k \geq 3$.

Claim 8. $I(\mathcal{P})$ *can contain the graphs* J_k'' *for all* $k \geq 3$.

Recall from Fig. 1 that J_k'' is composed of an induced path $(a, 2, \ldots, 2k-1, b)$, node 1 is adjacent to $a, 2, \ldots, 2k-1$, node $2k$ is adjacent to $2, \ldots, 2k-1, b$, whereas 1 and $2k$ are non-adjacent.

We consider a $(k-1)$-tree G composed of two paths induced by $(u_0, u_1, \ldots, u_{2k-1})$ and $(v_1, \ldots, v_{2k})$ that are connected by the edges $u_i v_i$ for even i with $1 \leq i \leq 2k-1$. We can embed a set $\mathcal{P}$ of paths $P(i)$ with $I(\mathcal{P}) = J_k''$ in such a network G, where

index k	origin o_k	destination d_k	weight w_k	path P_k
1	2	11	3	$2 \overset{l_1}{\to} 3 \overset{l_5}{\to} 6 \overset{l_{12}}{\to} 7 \overset{l_{15}}{\to} 11$
2	2	10	2	$2 \overset{l_2}{\to} 1 \overset{l_8}{\to} 9 \overset{l_{11}}{\to} 10$
3	3	15	5	$3 \overset{l_5}{\to} 6 \overset{l_{12}}{\to} 7 \overset{l_{13}}{\to} 8 \overset{l_{22}}{\to} 15$
4	2	5	4	$2 \overset{l_1}{\to} 3 \overset{l_5}{\to} 6 \overset{l_6}{\to} 5$
5	4	10	6	$4 \overset{l_7}{\to} 5 \overset{l_{10}}{\to} 10$
6	5	8	2	$5 \overset{l_4}{\to} 8$
7	4	9	3	$4 \overset{l_9}{\to} 9$
8	6	11	4	$6 \overset{l_{12}}{\to} 7 \overset{l_{15}}{\to} 11$
9	10	12	3	$10 \overset{l_{24}}{\to} 15 \overset{l_{23}}{\to} 14 \overset{l_{19}}{\to} 12$
10	1	6	5	$1 \overset{l_3}{\to} 4 \overset{l_7}{\to} 5 \overset{l_6}{\to} 6$
11	2	5	3	$2 \overset{l_1}{\to} 3 \overset{l_4}{\to} 4 \overset{l_7}{\to} 5$
12	4	6	3	$4 \overset{l_4}{\to} 3 \overset{l_5}{\to} 6$
13	8	10	3	$8 \overset{l_{14}}{\to} 5 \overset{l_{10}}{\to} 10$
14	10	6	3	$10 \overset{l_{10}}{\to} 5 \overset{l_6}{\to} 6$
15	3	8	3	$3 \overset{l_5}{\to} 6 \overset{l_{12}}{\to} 7 \overset{l_{13}}{\to} 8$
16	4	3	3	$4 \overset{l_4}{\to} 3$
17	5	7	3	$5 \overset{l_6}{\to} 6 \overset{l_{12}}{\to} 7$
18	6	2	3	$6 \overset{l_5}{\to} 3 \overset{l_1}{\to} 2$
19	7	12	3	$7 \overset{l_{15}}{\to} 11 \overset{l_{17}}{\to} 12$
20	8	9	3	$8 \overset{l_{14}}{\to} 5 \overset{l_7}{\to} 4 \overset{l_9}{\to} 9$

Table 1: The considered set of demands together with the selected routes

- $P(1) = (u_0, u_1, \ldots, u_{2k-1})$,
- $P(a) = (u_0, u_1, v_1)$,
- $P(2\ell) = (u_{2\ell}, u_{2\ell-1}, v_{2\ell-1}, v_{2\ell})$ for $1 \leq \ell \leq k-1$,
- $P(2\ell+1) = (u_{2\ell}, u_{2\ell+1}, v_{2\ell+1}, v_{2\ell}, v_{2\ell-1})$ for $1 \leq \ell \leq k-1$,
- $P(b) = (u_{2k-1}, v_{2k-1}, v_{2k})$, and
- $P(2k) = (v_1, \ldots, v_{2k})$.

Thus, for any $k \geq 3$, we have $I(\mathcal{P}) = J''_k$, see Fig. 29 for an illustration. $\Diamond$

Claim 9. *$I(\mathcal{P})$ can contain even antiholes $\overline{C}_{2k}$ for all $k \geq 4$.*

To represent even antiholes $\overline{C}_{2k}$ having nodes $1, 2, \ldots, 2k$ and the non-edges $i(i+1)$ for all $1 \leq i \leq 2k \bmod k$ as EPN graphs, we use the following 3-tree G to embed the paths.

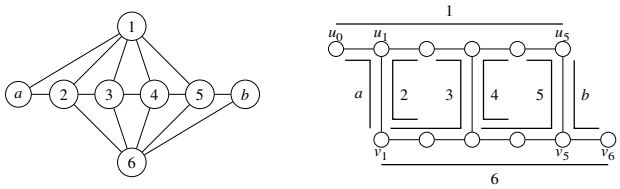

Figure 29: The EPN graph $J_3'' = I(\mathcal{P})$ with $\mathcal{P}$ in a network.

G has $\{v_1, v_2, \ldots, v_{2k+1}, u\}$ as node set and

$$\{v_i v_{i+1} : \ i \in \{1, \ldots, 2k\}\} \cup \{v_{2k+1}v_1, v_1 v_k, v_1 u, v_{2k+1}u\}$$

as edge set. That is $v_1, v_2, \ldots, v_{2k+1}$ induce in G a cycle C with exactly one chord $v_1 v_k$ and u has v_1 and v_{2k+1} as only neighbors. We define the following paths $P(i)$ in G (where all arithmetic are considered modulo $(2k + 1)$):

- $P(1) = (u, v_1, v_2, \ldots, v_k)$,
- $P(i) = (v_{(i-1)k}, v_{(i-1)k+1}, \ldots, v_{ik})$ for $2 \leq i \leq 2k - 2$,
- $P(2k - 1) = (v_{(2k-2)k}, \ldots, v_{2k+1}, u, v_1)$, and
- $P(2k) = (v_{2k+1}, v_1, v_k, v_{k+1}, v_{k+2})$.

Note that $P(1)$ and $P(2k - 1)$ are the only paths in $\mathcal{P}$ containing node u, $P(2k)$ is the only path in $\mathcal{P}$ containing edge $v_1 v_k$, and each path $P(i)$ for $2 \leqslant i \leqslant 2k - 2$ uses k consecutive edges of G in such a way that $P(i)$ ends at this node of C where $P(i + 1)$ starts (in clock-wise order on C). Hence, $I(\mathcal{P}) = \overline{C}_{2k}$ indeed holds for all $k \geq 4$ (see Fig. 30 for an illustration). □

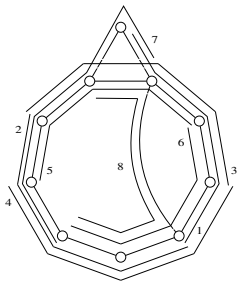

Figure 30: Illustration of the described path representation for $\overline{C}_8$ as edge intersection graph of paths over a 3-tree.

Fig. 31 shows non-basic minimal non-superperfect EPN graphs G and G' containing $\overline{A}_7$ and $\overline{A}_9$, resp.: they are non-superperfect (due to the indicated weight vectors causing a gap between weighted clique and interval chromatic number), they are minimal (as they do not have a non-comparability subgraph different from $\overline{A}_7 = G - g = G - h$ and $\overline{A}_9 = G' - h$, resp.), they are EPN graphs (see the according path representations).

However, note that neither G is an EPT graph (as $\overline{A}_7$ is not), nor an EPC graph (as nodes a, e, f, g, h induce a $K_{2,3}$ which is a non-circular-arc graph, see e.g. [5]), and G' is neither an EPT graph (as nodes b, c, d, f, g, h induce a G_1 which is a non-EPT graph by [9]) nor an EPC graph (as nodes a, c, d, f, h induce a $K_1 \cup C_4$ which is a non-circular-arc graph, see e.g. [5]).

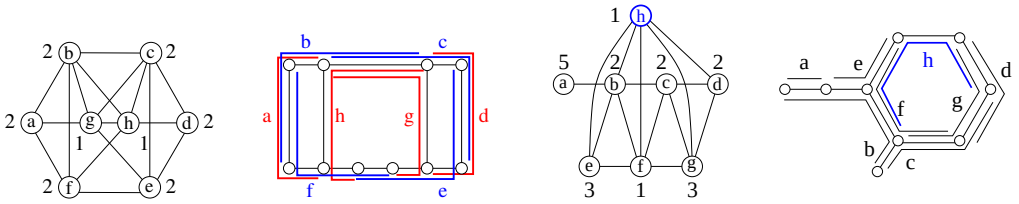

Figure 31: Non-basic minimal non-superperfect EPN graphs G (on the left) and G' (on the right) containing $\overline{A}_7 = G - g = G - h$ and $\overline{A}_9 = G' - h$, resp.

In view of the result by [10] that $I(\mathcal{P})$ can be *any* graph if G is a sufficiently large grid, we expect that *all* minimal non-superperfect graphs can occur in edge intersection graphs of paths in networks, as soon as the networks G satisfy minimal survivability conditions concerning edge or node failures.

7. Concluding remarks

In this work, we studied the question which minimal non-superperfect graphs can occur in edge intersection graphs $I(\mathcal{P})$ of routing paths $\mathcal{P}$ in flexgrid elastic optical networks. We considered several cases: when the optical network is a path, a tree, a cycle, or a sparse planar graph with small maximum degree, resp., and the edge intersection graphs $I(\mathcal{P})$ are accordingly EPP graphs, EPT graphs, EPC graphs, or EPN graphs, resp. In all cases, we characterized which basic minimal non-superperfect graphs can occur, see Theorem 3, 6, 9, 12. In addition, we discussed which minimal non-comparability superperfect graphs can occur as proper induced subgraphs of non-basic minimal non-superperfect graphs, see Lemma 4, 7, 11, 14, and exhibited examples of non-basic minimal non-superperfect graphs in the studied classes and, thus, several new examples of minimal non-superperfect graphs.

In particular, even in the most restricted case when the optical network is a path and the edge intersection graphs are interval graphs, non-superperfect edge intersection graphs $I(\mathcal{P})$ can occur and can cause a gap between $\omega(I(\mathcal{P}), \mathbf{w})$ and $\chi_I(I(\mathcal{P}), \mathbf{w})$ and, thus, also between the lower bound $\omega(G, \mathcal{D})$ and the minimum spectrum width $\chi_I(G, \mathcal{D})$. This is in accordance with the fact that the SA problem has been showed to be NP-hard on paths [20].

Hence, in all networks, it depends on the weights $\mathbf{w}$ induced by the traffic demands whether there is a gap between the weighted clique number $\omega(I(\mathcal{P}), \mathbf{w})$ and the interval chromatic number $\chi_I(I(\mathcal{P}), \mathbf{w})$. To determine the size of this gap, we propose to extend the concept of χ-binding functions introduced in [11] for usual coloring to interval coloring in weighted graphs, that is, to χ_I-binding functions f with

$$\chi_I(I(\mathcal{P}), \mathbf{w}) \leq f(\omega(I(\mathcal{P}), \mathbf{w}))$$

for edge intersection graphs $I(\mathcal{P})$ in a certain class of networks and all possible non-negative integral weights $\mathbf{w}$.

It is clearly of interest to study such χ_I-binding functions for different families of minimal non-superperfect graphs and to identify a hierarchy of graph classes between trees respectively cycles and sparse planar graphs resembling the structure of modern optical networks in terms of the gap between $\omega_I(I(\mathcal{P}), \mathbf{w})$ and $\chi_I(I(\mathcal{P}), \mathbf{w})$. Possible graph classes being of interest in this context are cacti (that are graphs where all cycles are edge-disjoint) and k-trees (that are graphs obtained from a tree by adding k edges) as common superclasses of trees and cycles.

Furthermore, in networks different from trees, the routing part of the RSA problem is crucial and raises the question whether it is possible to select the routes in $\mathcal{P}$ in such a way that neither non-superperfect subgraphs nor unnecessarily large weighted cliques (i.e., cliques Q with a weight $\mathbf{w}(Q) > \omega(G, \mathcal{D})$) occur in $I(\mathcal{P})$.

Finally, giving a complete list of minimal non-superperfect graphs is an open problem, so that our future work comprises to find more minimal non-superperfect graphs and to examine the here addressed questions for them.

Acknowledgment. We would like to thank Martin C. Golumbic and Martin Safe for interesting discussions on the topic, in particular concerning EPT graphs and circular-arc graphs.

References

[1] Andreae, T., *On superperfect noncomparability graphs*, J. of Graph Theory **9** (1985), 523–532.
[2] Berge, C., *Les problèmes de coloration en théorie des graphes*, Publ. Inst. Statist. Univ. Paris 9 (1960), 123–160.
[3] Christodoulopoulos, K., I. Tomkos and E. Varvarigos: *Elastic bandwidth allocation in flexible OFDM based optical networks*, IEEE J. Lightwave Technol. **29** (2011), 1354–1366.
[4] Chudnovsky, M., N. Robertson, P. Seymour, and R. Thomas, *The Strong Perfect Graph Theorem*, Annals of Mathematics **164** (2006), 51–229.
[5] Durán, G., L.N. Grippo and M.D. Safe, *Structural results on circular-arc graphs and circle graphs: A survey and the main open problems*, Discrete Applied Mathematics **164** (2014), 427–443.
[6] Fayez, M., I. Katib, G.N. Rouskas and H.M. Faheem, *Spectrum Assignment in Mesh Elastic Optical Networks*, IEEE Proc. of ICCCN (2015), 1–6.
[7] Gallai, T., *Transitiv orientierbare Graphen*, Acta Math. Acad. Sci. Hungar. **18** (1967), 25–66.
[8] Golumbic, M., *Algorithmic Graph Theory and Perfect Graphs*, 2nd Ed., North Holland, 2004.
[9] Golumbic, M., R. Jamison, *The Edge Intersection Graphs of Paths in a Tree*, J. Comb. Theory B **38** (1985) 8–22.
[10] Golumbic, M., M. Lipshteyn, M. Stern, *Edge intersection graphs of single bend paths in a grid*, Networks **54** (2009) 130–138.
[11] Gyárfás, A., *Problems from the world surrounding perfect graphs*, Zastos. Mat. **19** (1987), 413–431.
[12] Hajös, G., *Über eine Art von Graphen*, Int. Math. Nachr. **11** (1957), Problem 65.
[13] Hoffman, A., *A generalization of max flow-min cut*, Math. Prog. **6** (1974), 352–359.
[14] Kerivin, H. and A.R. Mahjoub, *Design of survivable networks: A survey*, Networks **46** (2005), 1–21.
[15] Kerivin, H. and A. Wagler, *On superperfection of edge intersection graphs of paths*, In: Graphs and Combinatorial Optimization: from Theory to Applications, C. Gentile et al. (Ed.). AIRO Springer Series 5 (2020) 79–91
[16] Lekkerkerker, C. and D. Boland, *Representation of finite graphs by a set of intervals on the real line*, Fundamenta Mathematicae **51** (1962), 45–64.
[17] Marenco, J. and A. Wagler, *On the combinatorial structure of chromatic scheduling polytopes*, Discrete Applied Mathematics **154** (2006), 1865–1876.
[18] Ozdaglar, A. and D. Bertsekas, Routing and wavelength assignment in optical networks, IEEE/ACM Trans. Netw. 11 (2003), pp. 259–272.
[19] Ruiz, M., M. Pioro, M. Zotkiewicz, M. Klinkowski, and L. Velasco, *Column generation algorithm for RSA problems in flexgrid optical networks*, Photonic Network Communications **26** (2013), 53–64.
[20] Shirazipourazad, S., Ch. Zhou, Z. Derakhshandeh and A. Sen: *On routing and spectrum allocation in spectrum sliced optical networks*, Proceedings of IEEE INFOCOM (2013), 385–389.
[21] Talebi, S., F. Alam, I. Katib, M. Khamis, R. Salama, and G.N. Rouskas: *Spectrum management techniques for elastic optical networks: A survey*, Optical Switching and Networking **13** (2014), 34–48.
[22] Wang, Y., X. Cao and Y. Pan: *A study of the routing and spectrum allocation in spectrum-sliced elastic optical path networks*, in: Proceedings of IEEE INFOCOM 2011, 1503-1511.